JOURNAL OF DIFFERENTIAL EQUATIONS 119, 284–309 (1995)

The Collinear Three-Body Problem with Negative Energy

KENNETH MEYER* AND QUIDONG WANG

Institute of Dynamics, Department of Mathematics, University of Cincinnati, Cincinnati, Ohio 45221

Received April 15, 1993; revised November 15, 1993

The geometry of the global phase space of the collinear three-body problem with negative energy is presented in this paper. A set of transformations is introduced to create fictitious boundaries to make the phase space compact. At first, the binary collisions are not regularized. Then one of the binary collisions (the collision between m_2 and m_3) is regularized and we analyze the phase structure of this "half regularized" system. Finally, the second binary collision (the collision between m_1 and m_2) is regularized and we analyze how the phase structure is transformed by this regularization. The whole analysis provides a vivid picture of the phase flow of the collinear three-body problem. © 1995 Academic Press, Inc.

Consider the dynamics of three particles moving on a line where the interactions among particles obey the Newtonian gravitational law. This collinear three-body problem is a two degree of freedom problem with total energy as an integral. Thus fixing energy reduces the problem to a three dimensional manifold. Since we are interested in triple collisions we will restrict our study to the case where the energy is negative. The flow is relatively simple if the binary collisions are not regularized. Every solution will end in a collision, either binary or triple. The solutions of triple collision separate the phase space into regions of different binary collisions.

Things become interesting after the binary collisions are regularized. The analyze of this problem uses symbolic dynamics because of the presence of heteroclinic phenomenon. The first example of a unbounded solutions in finite time [1] and of a super-hyperbolic motion [2] were given based on the study of this problem.

The discussion in this paper follows the line of [3] and [4] where we developed a method to study the phase structure of gravitational models. We are mostly concerned with the global geometry of the phase structure not just particular solutions with special properties. The symbolic systems created by others [2] will come out as a natural by-product. Even for

* This research partially supported by grants from the NSF.

0022-0396/95 $12.00

relatively simple systems such as the collinear three-body problem without regularized binary collisions, questions about the phase structure are usually interesting and non-trivial. For example, we may ask how the solutions of triple collision separate the phase space into regions, what is the geometry of these regions, and how they fit together in phase space.

We will divide our analysis three steps. At first we do not regularize the binary collisions. A set of transformations is introduced to create fictitious boundaries to make the phase space compact. Then we regularize one of the binary collisions (the collision between m_2 and m_3) and analyze the phase structure of this "half regularized" system. Finally, we regularize the second binary collision (the collision between m_1 and m_2) to see how the phase structure is transferred by this regularization. The method developed in this paper is general and can be used to study other gravitational systems with two degrees of freedom.

I. The Compact Phase Space before Regularizing Binary Collisions

Three particles, m_1, m_2, m_3, are on a line with coordinates x_1, x_2, x_3 respectively with $x_1 < x_2 < x_3$. The system has potential function

$$U = \frac{m_1 m_2}{r_{12}} + \frac{m_2 m_3}{r_{23}} + \frac{m_1 m_3}{r_{13}},$$

where $r_{12} = x_2 - x_1$, $r_{13} = x_3 - x_1$, $r_{23} = x_3 - x_2$.

The equations of motion are

$$dq/dt = M^{-1}p, \qquad dp/dt = \nabla U(q),$$

where $q = (x_1, x_2, x_3)^T$, $M = \mathrm{diag}(m_1, m_2, m_3)$. We can fix the center of mass at the origin and set total linear momentum to zero, i.e.

$$m_1 x_1 + m_2 x_2 + m_3 x_3 = 0$$

$$p_1 + p_2 + p_3 = 0.$$

The system admits the integral of energy

$$p^T M^{-1} p/2 - U(q) = h.$$

We will only consider the case of $h < 0$, since we are interested in triple collisions.

In order to compactify phase space we use the series of coordinate changes introduced in [5]. Let

$$u^{-1} = 2U(q), \qquad F = u^{-1}q, \qquad G = u^{1/2}p, \qquad dt/d\tau = u^{3/2},$$

so (u, F, G, t) satisfy

$$\begin{aligned} du/d\tau &= -2(M^{-1}G, \nabla U(F))\, u \\ dF/d\tau &= M^{-1}G + 2(M^{-1}G, \nabla U(F))\, F \\ dG/d\tau &= \nabla U(F) - (M^{-1}G, \nabla U(F))\, G \end{aligned} \tag{1.1}$$

and the constraints

$$G^T M^{-1} G = 1 + 2uh \tag{1.2}$$

$$1/2 - U(F) = 0 \tag{1.3}$$

as well as the integral of momentums

$$m_1 F_1 + m_2 F_2 + m_3 F_3 = 0, \qquad G_1 + G_2 + G_3 = 0. \tag{1.4}$$

There are seven equations and four constraints, so the problem can be reduced to three dimensions. The first step is to get rid of (1.4) by introducing

$$\begin{aligned} Y_1 &= F_2 - F_1, & Z_1 &= G_2/m_2 - G_1/m_1 \\ Y_2 &= F_3 - F_2, & Z_2 &= G_3/m_3 - G_2/m_2 \end{aligned} \tag{1.5}$$

so that

$$\begin{aligned} G_1 &= -m_1(m_3 Z_2 + (m_2 + m_3)\, Z_1)/(m_1 + m_2 + m_3) \\ G_2 &= m_2(m_1 Z_1 - m_3 Z_2)/(m_1 + m_2 + m_3) \\ G_3 &= m_3(m_1 Z_1 + (m_1 + m_2)\, Z_2)/(m_1 + m_2 + m_3) \end{aligned} \tag{1.6}$$

and

$$\begin{aligned} P &= (M^{-1}G, \nabla U(F)) \\ &= -(m_1 m_2 Z_1/Y_1^2 + m_2 m_3 Z_2/Y_2^2 + m_1 m_3 (Z_1 + Z_2)/(Y_1 + Y_2)^2). \end{aligned} \tag{1.7}$$

The differential equations for the new variables are

$$\begin{aligned} du/d\tau &= -2Pu \\ dY_1/d\tau &= Z_1 + 2PY_1 \\ dY_2/d\tau &= Z_2 + 2PY_2 \\ dZ_1/d\tau &= -(m_1 + m_2)/Y_1^2 + m_3/Y_2^2 - m_3/(Y_1 + Y_2)^2 - PZ_1 \\ dZ_2/d\tau &= -(m_2 + m_3)/Y_2^2 + m_1/Y_1 - m_1/(Y_1 + Y_2)^2 - PZ_2 \end{aligned}$$

and the constraints are

$$T(Z_1, Z_2) + 2u|h| = 1 \tag{1.8}$$

$$1/2 - U(Y_1, Y_2) = 0. \tag{1.9}$$

P is defined by (1.7) and $T(Z_1, Z_2)$ is defined by $T = G^T M^{-1} G$ and (1.6). T is a positive definite quadratic form in Z_1 and Z_2.

We will eliminate (1.9) by introducing

$$Y_1 = r \sin\theta, \qquad Y_2 = r\cos\theta, \qquad Z_3 = u^{1/2}.$$

The angle θ measures the ratio of the distance between m_2 and m_1 to the distance between m_3 and m_2. For any real solution of this system, we see that $\theta \in (0, \pi/2)$ and $Z_3 > 0$. By (1.9)

$$r = 2\Psi(\theta)/(\sin\theta\cos\theta(\sin\theta + \cos\theta)),$$

$$\Psi(\theta) = m_1 m_2 \cos\theta(\sin\theta + \cos\theta) + m_3 m_2 \sin\theta(\sin\theta + \cos\theta) + m_1 m_3 \cos\theta \sin\theta,$$

so

$$P = -[Z_1 m_1 m_2 \cos^2\theta(\sin\theta + \cos\theta)^2 + Z_2 m_3 m_2 \sin^2\theta(\sin\theta + \cos\theta)^2 + (Z_1 + Z_2) m_1 m_3 \cos^2\theta \sin^2\theta]/4\Psi^2(\theta). \tag{1.10}$$

The equations for (θ, Z_1, Z_2, Z_3) are

$$\begin{aligned}
d\theta/d\tau &= \sin\theta\cos\theta(\sin\theta + \cos\theta)(Z_1\cos\theta - Z_2\sin\theta)/2\Psi(\theta)\\
dZ_1/d\tau &= [-(m_1 + m_2)\cos^2\theta(\sin\theta + \cos\theta)^2\\
&\quad + m_3 \sin^2\theta(\sin\theta + \cos\theta)^2\\
&\quad - m_3 \cos^2\theta \sin^2\theta]/4\Psi^2(\theta) - PZ_1\\
dZ_2/d\tau &= [m_1 \cos^2\theta(\sin\theta + \cos\theta)^2\\
&\quad - (m_3 + m_2)\sin^2\theta(\sin\theta + \cos\theta)^2\\
&\quad - m_1 \cos^2\theta \sin^2\theta]/4\Psi^2(\theta) - PZ_2\\
dZ_3/d\tau &= -PZ_3
\end{aligned} \tag{1.11}$$

These variables satisfy the constraint

$$T(Z_1, Z_2) + 2|h| Z_3^2 = 1. \tag{1.12}$$

Now the domain of these equations has been extended to $\theta = 0, \pi/2$ and $Z_3 = 0$.

Now we will look at the flow on the boundary. Topologically, (1.12) defines a two-dimensional disk D^2 in (Z_1, Z_2, Z_3) space with the circle S^1 where $Z_3 = 0$ as its boundary (recall that T is positive definite.) So the extended phase space is the cylinder $D^2 \times I$, where $I = [0, \pi/2]$. Refer to Figure 1.

Equation (1.11) defines non-trivial flows on the boundaries of this cylinder. Now we will study the flow on these boundaries. When $\theta = 0$, the equations for (Z_1, Z_2, Z_3) are

$$dZ_1/d\tau = (-(m_1 + m_2)/m_1 m_2 + Z_1^2)/4m_2 m_1$$
$$dZ_2/d\tau = (1/m_2 + Z_1 Z_2)/4m_2 m_1$$
$$dZ_3/d\tau = Z_1 Z_3/4m_2 m_1$$

with

$$T(Z_1, Z_2) + 2|h| Z_3^2 = 1$$

This last constraint implies $Z_1^2 \leqslant (m_1 + m_2)/m_1 m_2$ and hence $dZ_1/dt \geqslant 0$. It is now easily to see that there are two critical points and that Figure 2 gives for the phase portrait for this boundary. For the case of $\theta = \pi/2$, the picture is similar.

The rest of the boundary corresponds to $Z_3 = 0$ (recall that when $Z_3 = 0$, $U(q) = \infty$, so it is the collision manifold). By setting $Z_3 = 0$ in equations (1.11)–(1.13), we have:

$$d\theta/d\tau = \sin\theta \cos\theta(\sin\theta + \cos\theta)(Z_1 \cos\theta - Z_2 \sin\theta)/2\Psi(\theta),$$
$$dZ_1/d\tau = [-(m_1 + m_2)\cos^2\theta(\sin\theta + \cos\theta)^2$$
$$+ m_3 \sin^2\theta(\sin\theta + \cos\theta)^2$$
$$- m_3 \cos^2\theta \sin^2\theta]/4\Psi^2(\theta) - PZ_1,$$
$$dZ_2/d\tau = [m_1 \cos^2\theta(\sin\theta + \cos\theta)^2$$
$$- (m_3 + m_2)\sin^2\theta(\sin\theta + \cos\theta)^2$$
$$- m_1 \cos^2\theta \sin^2\theta]/4\Psi^2(\theta) - PZ_2,$$

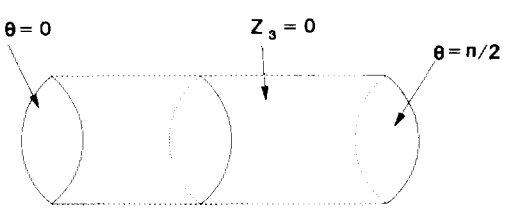

FIG. 1. The phase space.

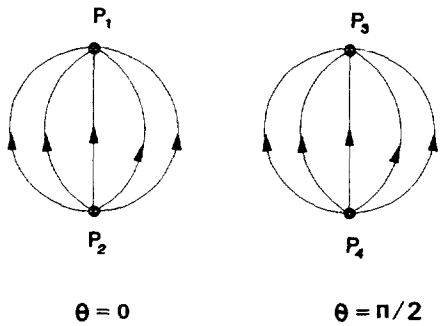

FIG. 2. The boundary of the degenerate configuration.

as well as

$$T(Z_1, Z_2) = 1$$

It is not necessary for us to do a detailed analysis of the phase portrait on the collision manifold, since the flow here is equivalent to the flow that was obtained in McGehee [6]. The only difference is that, instead of regularizing, we introduced sub-collision manifold for binary collisions.

Refer to the Figure 3 for the entire picture on the boundary of the phase space. The well-known flow on the McGehee manifold is illustrated in Figure 6. The lines l_1 and l_2 corresponds to binary collisions. To obtain our Figure 3 from McGehee's Figure 6 (i) cut the manifold alone the lines l_1 and l_2 to obtain four lines (ii) collapse each of these four lines to a point to obtain the points P_1, P_2, P_3, P_4 (this gives the cylinder side of Figure 6) (iii) now add the two disks depicted in Figure 2 to ends of the cylinder.

In Figure 3, $P_1, P_2, P_3, P_4, E_j, E_c$ are rest points. P_1, P_3 are sinks and P_2, P_4 are sources. All the solutions of binary collision of m_1 and m_2 tend to P_1 and all the solutions of binary ejection of these two start from P_2. Similarly, P_3 represents the collision of m_2 and m_3, and P_4, the ejection of them.

E_c and E_j are hyperbolic fixed points corresponds to the Euler collinear central configuration. E_c has a two-dimensional stable manifold inside of

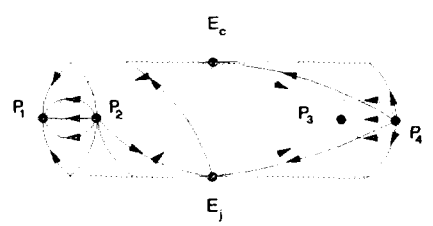

FIG. 3. The flow on the boundary of the phase space.

the phase space and one-dimensional unstable manifold on the collision boundary. Similarly, E_j has two-dimensional unstable manifold inside and one dimensional stable manifold on the boundary. Physically, all the real solutions of triple collision form the stable manifold of E_c and that of triple ejection form the unstable manifold of E_j.

As we mentioned before, solutions inside of phase space will start from one of the ejection points and end in one of the collision points. The triple collision solutions form a two dimensional embedded manifold inside phase space. This manifold divides the three-dimensional phase space into regions of solutions of different binary collisions.

Now consider the flow inside the phase space. The phase space is a cylinder (see Figure 3). Think that the boundary $\theta = 0$ is the base and the collision manifold is the side of the cylinder.

Refer to Figure 4. Take a sufficiently small sphere (two dimensional surface) centered at P_2 and denote the intersection of this sphere with the boundary $\theta = 0$ by 1 and that of the sphere with the collision manifold by 1'. Call the portion of the sphere, which is in the phase space, S. We see that S is an quarter-sphere with 1 and 1' as its boundary. Denote the interior of S by S^* ($= S \setminus (1 \cup 1')$).

Since P_2 is an source, we can chose the sphere such that it is transversal to the vector field so all the vectors are pointing outward on S. Let $W^s(P)$ and $W^u(P)$ denote the stable and unstable manifold respectively of a hyperbolic fixed point P and

$$A = S \cap W^s(P_1), \qquad W = S \cap W^s(P_3), \qquad C = S \cap W^s(E_c).$$

We see that $(A \cup W \cup C) \cap S^* = S^*$. The solutions starting from A will end in a binary collision of m_1 and m_2 and those starting from W will end in a binary collision of m_2 and m_3. Likewise, the solutions starting from C will end in a triple collision.

LEMMA 1.1. (a) *For any $p \in A$ (or W), there is a neighborhood $U(p)$ of p in S such that $U(p) \subseteq A$ (or W).*

(b) *C consists of one-dimensional curves in S^*.*

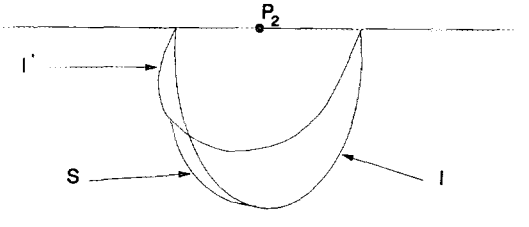

FIG. 4. The surface around P_2.

Proof. Part (a) is true since P_1 and P_3 are sources. Part (b) is true since $W^s(E_c)$ is a two-dimensional embedded manifold inside of the phase space transversal to the surface S. ∎

Given an open arc in S^* we will chose a parameterization by giving a map $c(t)$: $(-\infty, +\infty) \to S^*$. The choice of parametrization is arbitrary. Define the α-limit and ω-limit set of an arc given parametrically by $c(t)$: $(-\infty, +\infty) \to S^*$ by

$$\alpha = \{p \in S: \text{there exist } t_n \to -\infty, \text{ such that } c(t_n) \to p\}$$

and

$$\omega = \{p \in S: \text{there exists } t_n \to +\infty, \text{ such that } c(t_n) \to p\}.$$

We also say $c(t)$ connects α and ω and that α and ω are limit points of c.

Take a path connected branch B of C in S^*. B is not a circle inside of S^* since it is the intersection of a two dimensional stable manifold and a transverse cross section. Similarly, B has no limit point inside of S^* or on the boundary 1. Therefore, only 1′, the intersection of S with the collision-boundary, contains the limit points of B.

Refer to Figure 5. There are two special points Q_1, Q_2 on 1′, namely $Q_1 \in W^s(E_j)$ and $Q_2 \in W^s(E_c)$. The segments aQ_1, Q_2b of 1′ are in A and the segment Q_1Q_2 is in W, see Figure 3 also. So Q_1, Q_2 are the only candidates for the limit point of B. Because the $\omega(\alpha)$-limit set has to be connected in S, the limit set has to be either Q_1 or Q_2.

We call a branch B of C a *regular branch* if B connects Q_1 and Q_2; otherwise, we call it a *loop*.

LEMMA 1.2. *There is one and only one regular branch. It is also the only branch of C, which has Q_2 as its limit set.*

P_1 and P_3 are sinks so the sets of the points tending to them are open and therefore A and W are open in S. A and W must be separated by C.

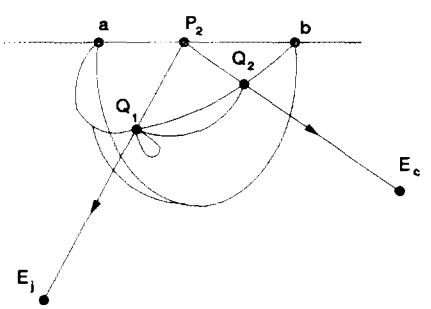

FIG. 5. The phase structure of the unregularized system.

Since segment Q_1Q_2 is in W and the segment aQ_1 is in A one component of C must connect Q_1 and Q_2 (a regular branch exist).

$W^s(E_c)$ is an embedded two-dimensional submanifold and $Q_2 \in W^s(E_c)$. Two branches of C having Q_2 as limit sets would contradict the local structure of $W^s(E_c)$ at E_c given by the stable manifold theorem.

The loop structure around Q_1 might be quite complicated, since it depends on the intersections of $W^u(E_j)$ and $W^s(E_c)$ which is a global feature. We will discuss it in detail in the next section, but a complete answer seems out of the question at present. This completes our discussion of the non-regularized system.

II. Regularization of One Binary and Character Number

According to McGehee [6], the triple collision manifold for the collinear three-body problem is shown in Figure 6.

The lines l_1, l_2 correspond to the binary collisions of m_1, m_2 and m_2, m_3 respectively. E_c and E_j are as before. On this two-dimensional surface, two branches of $W^u(E_c)$ are denoted as $\hat{\gamma}^+$ and $\hat{\gamma}^-$. In this picture, $\hat{\gamma}^+$ goes to l_2 first, and $\hat{\gamma}^-$ to l_1, then they will go back and forth between l_1 and l_2 and finally end up going up one of the arms. Assume $\hat{\gamma}^+$ goes to the left arm and $\hat{\gamma}^-$ the right arm. Also denote the number of times $\hat{\gamma}^+$ hits l_2 by μ. $\mu \geqslant 1$.

Consider the phase portrait in Figure 3. By regularizing the binary collision of m_2, m_3, we replace the right-half of the phase space by the right-half of the McGehee's manifold—interiors included. Therefore, the phase space looks like Figure 7.

Now the final evolution is changed for some trajectories in this half-regularized system. In fact, four kinds of final evolutions are possible for the solutions in the interior of the phase space:

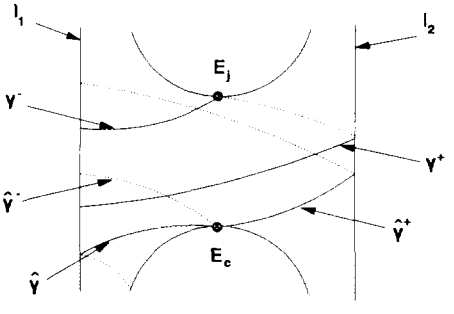

Fig. 6. The flow on the McGehee manifold.

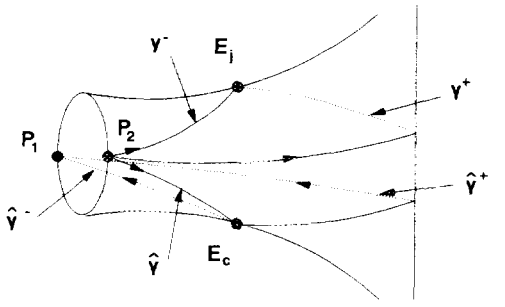

FIG. 7. The half-regularized phase space.

(a) It will tend to with binary collision between m_1 and m_2.

(b) It will tend to a triple collision.

(c) The particule m_1 will approach infinity with non-zero velocity (the hyperbolic solution).

(d) The particle m_1 will approach infinity with zero velocity (the parabolic solution).

We call a point p *hyperbolic* (or *parabolic*) if p is on a hyperbolic solution (or parabolic solution), otherwise we call the solution an *elliptic solution* and the corresponding points *elliptic points*. The following lemma is proved in [7].

LEMMA 2.1. (a) *The set of hyperbolic points is open.*

(*b*) *The set of parabolic solutions is the stable manifold of a periodic orbit at infinity and this manifold is real analytic. Furthermore, for any parabolic point p, and any neighbourhood* $U(p)$, *there are two points* p_1 *and* p_2, *in* $U(p)$ *such that* p_1 *is hyperbolic and* p_2 *is elliptic.*

For any point p inside of the phase space, let

$$\begin{aligned} O(\tau, p) &= \text{the solution at time } \tau \text{ which starts from } p \text{ at } \tau = 0; \\ O(p) &= \{O(\tau, p): 0 < \tau < \infty\}; \\ H &= \{p: p \text{ is a hyperbolic point}\}; \\ P &= \{p: p \text{ is a parabolic point}\}; \\ E &= \{p: p \text{ is an elliptic point}\}. \end{aligned} \tag{2.1}$$

Let $N(p) =$ number of the binary collisions of m_2, m_3 in the set $O(p)$. Call $N(p)$ the *character number* of p. $N(p) = \infty$ if p is hyperbolic or parabolic point. Otherwise, $N(p)$ is finite and the solution tends to either a binary collision of m_1, m_2 or triple collision.

Refer to Figures 7 and 8. As before, take a sphere around P_2 to obtain the surface S, its interior S^* and the two boundary curves 1 and 1'. On 1', the points a, b, Q_1, Q_2, are as before, but define the point Q_3 as the intersection of γ^+ with 1'. For $p \in aQ_1 \cup Q_2 b$, $N(p) = 0$; for $p \in Q_3 Q_2$, $N(p) = 1$; and for $p \in Q_1 Q_3$, $N(p) = \infty$. Also let

$$S^* \cap H = \Sigma_H, \qquad S^* \cap P = \Sigma_P, \qquad S^* \cap E = \Sigma_E. \tag{2.2}$$

Intuitively, Σ_P separate Σ_H and Σ_E in S^*.

LEMMA 2.2. (a) *Σ_P consists of one-dimensional curves in S.*

(b) *For any $B \in \Sigma_P$, a path connected branch of Σ_P, containing B is either a regular branch connecting Q_1, Q_3 or a loop taking both of its limit sets as Q_1 or Q_3.*

(c) *Σ_P, locally separates S^*; on one side $N(p) = \infty$ and on the other side $N(p) < \infty$.*

Proof. (a) and (c) are direct consequences of Lemma 2.1. The argument for (b) is similar to the corresponding argument given in the first section. ∎

Let $\Sigma = S^* \cap W^s(E_c)$.

LEMMA 2.3. (a) *Σ consists of one-dimensional curves in S^*.*

(b) *Given $p \in \Sigma$, there is a neighborhood $U(p)$ of p in S^*, such that $N(p) \leqslant N(q) \leqslant N(p) + 1$ for any $q \in U(p)$. Furthermore, there are $q_1, q_2 \in U(p)$, such that $N(q_1) = N(p)$ and $N(q_2) = N(p) + 1$.*

(c) *For any path connected component B of Σ in S^*, B is either a regular branch connecting two of the points Q_1, Q_2, Q_3 or a loop around Q_1*

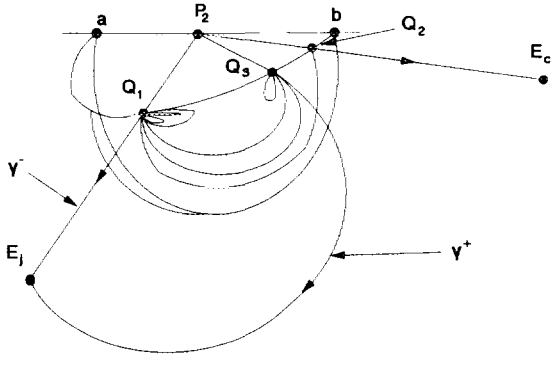

FIG. 8. The geometric structure on S.

or Q_3. Furthermore, there is only one branch which is ends at Q_2. It connects Q_1 and Q_2.

Proof. Parts (a) and (c) follow from an argument similar the argument given in the first section.

$p \in \Sigma$ is a point on the stable manifold of E_c so the flow will take any neighborhood of p arbitrarily close to the unstable manifold of E_c by the λ-lemma. Some points of the neighborhood will follow $\hat{\gamma}^+$ and experience an additional binary collision before approaching the sink P_1 and some will follow $\hat{\gamma}^-$ and be attracted straight to the sink P_1. For those points q that follow $\hat{\gamma}^+$ we have $N(q) = N(p) + 1$ and those that follow $\hat{\gamma}^-$ we have $N(q) = N(p)$. See Figure 7. ∎

According to Lemmas 2.2 and 2.3, $\Sigma \cup \Sigma_P$ divides S^* into mutually disjoint regions with different character number N. This will give a very rich geometric structure on S^* which is our primary object to study.

We will call a path connected component of $S^* \backslash (\Sigma \cup \Sigma_P)$ a *unit*. If a unit has a regular branch for one boundary we call it a *strip*, otherwise, we call it a *ring*. We note that a strip will have two and only two regular branches in its boundary. The boundary of a ring will contain an outer-loop and, may be, a bunch of inner-loops as shown in Figure 9. If an ring has no inner loop, we call it a simple ring.

PROPOSITION 2.1. (a) *$N(p)$ is constant on a unit.* (b) *For any integer $k \geqslant 0$, there exists a strip in S, such that the character number of this strip is k.*

Proof. Since the character nummber can change only on the points of $\Sigma \cup \Sigma_P$, part (a) is clear. Part (b) follows from part (a) of Lemma 2.3. ∎

From now on, we will use a triplet (k_1, k_2, k_3) to represent a unit, where $k_1 \leqslant k_3$ are the possible character numbers on the boundary of the unit and k_2 is the character number of interior of the unit.

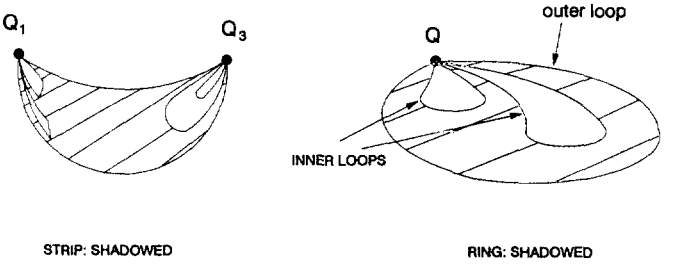

FIG. 9. Picture of units on S.

PROPOSITION 2.2. (a). *Units on S^* satisfies the restriction*:

$$k_1 \leqslant k_3 \leqslant k_2 \leqslant k_1 + 1.$$

That is, any unit on S^* has one of the following three representations: $(k, k+1, k+1)$; (k, k, k); $(k, k+1, k)$—*see Figure* 9.

(b) *For any given integer $k \geqslant 0$, there is a strip in form of $(k, k+1, k+1)$. Furthermore, the regular branches of its boundary have different character number.*

Proof. Part (a): $k_1 \leqslant k_3$ follows by definition of a triplet, $k_3 \leqslant k_2$ and $k_2 \leqslant k_1 + 1$ follow from Lemma 2.3. Part (b): The character number must increase from 0 to infinity, and Lemma 2.3(b) shows that the increment is at most one when crossing a boundary, so every integer must *be* obtained. Furthermore, the strip described in (b) is the only choice which will increment the character number globally. Therefore it must occur at least once for any $k \geqslant 0$. ∎

Ideally only the kind of strips described in (b) occur, in which case the character number of the strips will increase monotonically. In next section, we will study this case in detail, and show that, if this really happens, Σ_P will have no loops and the loop structure of Σ will be simple.

Now turn to the rings. First note that all loops form a partially ordered set by inclusion, i.e., if B_1 and B_2 are loops then we say $B_1 < B_2$ if B_1 is in the interior of B_2. So, for a given ring B, we always have $B_1 < B_0$, where B_1 is any inner-loop of B and B_0 is the outer-loop of B.

Take a strip U and a loop B_1 on S. We say that B_1 is confined by U either B_1 is on the boundary of U or $B_1 < B_u$, where B_u is on the boundary of U.

PROPOSITION 2.3. *Consider a strip with expression (k_1, k_2, k_3). If a parabolic loop $B \subset \Sigma_P$ is confined by the given strip, then*:

(a) *There exist infinite sequence $\{B_n\} \subset \Sigma$*:

$$B_1 > B_2 > \cdots > B_n > B_{n+1} > \cdots > B$$

(b) *For any integer $k > k_2$, there is a ring with expression $(k, k+1, k+1)$. This ring has a member of the sequence in* (a), *say B_i, as its outer-loop and B_{i+1} as part of its inner loop. Furthermore, the character number of B_i is k and that of B_{i+1} is $k+1$.*

The proof is similar to the proof of Proposition 2.2.

Now turn to the geometry of $W^s(E_c) \cap W^u(E_j)$ since the structure on S^* depends heavily on this intersection. The rest of this section is devoted to a discussion of this dependency. Since we are interested in the geometric picture, we will give a "geometric description" rather than a "formal definition and proof presentation". This will make the discussion easier to understand. However, one can add technical details to make the discussion formal and complete.

Assume $c(t): (-\infty, \infty) \to S^*$ is a given branch B of Σ and $\lim_{t \to \infty} c(t) = Q$. Since $W^s(E_c)$ is a real analytic manifold, B will be smooth at Q. Denote by $c^+ = \{c(t): t > M\}$, $c^- = \{c(t): t < -M\}$, where $M > 0$ is a large constant. We call c^+ and c^- the *tails* of the branch B. In general, we will denote a tail of B as $T(B)$ (or simply T). If T is c^+ and Q is the ω-limit of $c(t)$, we will say that T *is at* Q. Similarly, we also say T *is at* Q if T is c^- and Q is the α-limit. Note that we can take M arbitrarily large for the given B.

Refer to Figure 10. For two given tails T_1 and T_2 at Q_1, take a sphere U_q centered at Q_1, so $U_q \cap S^*$is a simple curve L. As in the picture, α_0, α_1 are the end points of L. We can make the radius of U_q so small that L intersect T_1 and T_2. Take $p_1 \in L \cap T_1$, $p_2 \in L \cap T_2$. We say $T_1 < T_2$ if p_1 is closer to α_0 on L than p_2. One sees that this definition gives a well-defined order between all the tails at Q_1 since they are smooth at Q_1 and are mutually disjoint.

We can do the same at E_j and define an order among all the orbit on $W^u(S^*)$. Refer to Figure 10, we see $l_1 < l_2$ where $l_1, l_2 \in W^u(E_j)$.

Refer to Figure 11. T is a tail at Q_1. Remember Q_1 is on γ^-, one of the branches of the stable manifold of E_j. T will first follow γ^+, then it will follow one of the orbits of the l_T on $W^u(E_j)$. Finally, its image is the segment T' in this picture.

A similar description can be given for the tails at Q_3. Since Q_3 is on γ^+, the other branch of $W^s(E_j)$, a tail T at Q_3 will first follow γ^+, reach the other side of $W^u(E_j)$, then follow one of the orbit l_T on $W^u(E_j)$.

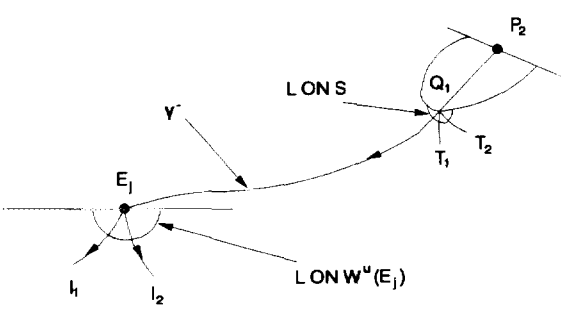

FIG. 10. The order on S and $W^u(E_j)$.

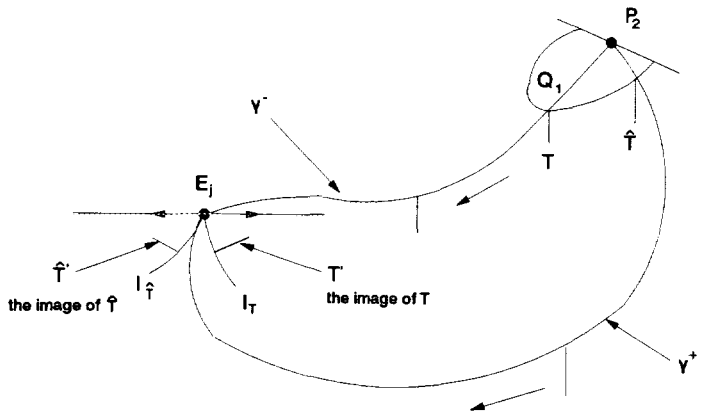

FIG. 11. The flow of tails under the flow.

PROPOSITION 2.4. (a) *Assume* T_1, T_2 *are tails at* Q_1 *(or* Q_3*),* $T_1 < T_3$, *and that* T_1 *follows* l_{T_1}, T_2 *follows* l_{T_2}, *where* $l_{T_1}, l_{T_2} \in W^u(E_j)$ *then* $l_{T_1} < l_{T_2}$.

(b) *For any given tail* T, $l_T \in W^u(E_j) \cap W^s(E_c)$.

(c) *For two tails* T^+ *and* T^- *of a loop* B *at* Q_1 *(or* Q_3*),* l_{T^+} *and* l_{T^-} *are different.*

Proof. The claim of part (a) is topological and can be checked in small neighborhood of E_j. So it is enough to check it for the linearized system at E_j which is readily done.

If (c) were not true the local structure of $W^s(E_c)$ at E_c would be destroyed. For (b), $l_T \in W^u(E_j)$ by definition. l_T must end up at E_c since all the points on T' do so and they have the same finite character number. If l_T ends up with P_1, a neighborhood of l_T, which will include points on T', will do the same. This is a contradiction. If l_T ends up with parabolic or hyperbolic final evolution, we will have infinitely large character number nearby l_T, which will contradict to the fact that the character number on T' is finite. ∎

Proposition 2.4(a) will be crucial for "reading off" the geometric structure from the intersection graph, which we are going to give next.

Refer to the part of $W^u(E_j)$ in Figure 10. To avoid tedious technique details, we will assume that $L \cap W^u(E_j) \cap W^s(E_c)$ is a discrete set. It will become clear when the discussion is finished that the whole argument can be modified when the intersection is more complicated.

Let H be the ε-neighborhood of L inside of the phase space where ε is sufficiently small—see the curve L around E_j in Figure 10. The local unstable manifold of E_j will divide H into two parts: H^+ and H^-. We call

H^+ the positive side and H^- the negative side of L. For any orbit l on $W^u(E_j)$, l intersect L once and only once.

Now refer to Figure 12. Take a curve L' in $W^s(E_c)$ near E_c, such that it intersects all of the solutions in $W^s(E_c)$ transversely. If $p \in L \cap W^u(E_j) \cap W^s(E_c)$, then there is a $p' \in L'$ with p and p' are on the same orbit.

Starting from p', go on the curve L' until another solution $l \in W^u(E_j) \cap W^s(E_c)$ is found. Let $p_1' = l \cap L'$ and the segment $p'p_1'$ on L be B'. By pulling B' backward under the flow, we will obtain another curve B_0 inside of the phase space, which connects p and p_1, where $p_1 = l \cap L$. Note that the interior of B_0 does not intersect $W^u(E_j)$.

There are three possible for B_0:

(1) The tails of B_0 at p and p_1 are both in H^+.

(2) The tails of B_0 at p and p_1 are both in H^-.

(3) The tail of B_0 at p is in H^+ (or H^-) and that of p_1 is in H^- (or H^+).

PROPOSITION 2.5. *Following the flow backward,* (1) *gives a loop at* Q_1, (2) *gives a loop at* Q_3 *and* (3) *gives a regular branch connecting* Q_1 *and* Q_3 *on* S^*.

Proof. Following the flow backward, we see that a tail of B_0 in H^+ follows γ^+ backward. This will give a tail at Q_1. Similarly, a tail of B_0 in H^- follows γ^-, and gives a tail at Q_3.

The flow is reversible. So we again have the four possible final evolutions listed at the beginning of this section when we follow the flow backward. We need to show that all the points on B_0 will end up with P_2. Note that on B_0, we have no points of triple ejection. So the only other option is a point p on B_0, such that the particle m_1 came from infinity for the solution

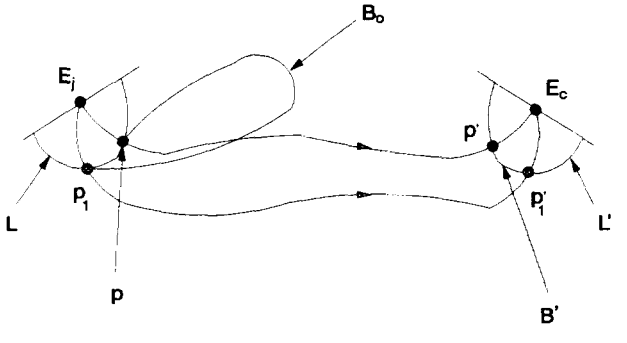

FIG. 12. The intersection of $W^u(E_j)$ and $W^s(E_c)$.

passing through p. Count the number of binary collision between m_2 and m_3 this solution experienced before p. It must be infinite. Now for nearby tails of B_0, this number must be finite. So it changes at some point of B_0. But such a point must be on $W^u(E_j)$, which is impossible. ∎

Now start from p_1', and go on L' in the given direction. We will meet another point p_2' of $W_j^u(E) \cap W_c^s(E)$. We can do the same pulling back operation for the new segment $p_1'p_2'$ as for the B' above. Keep going, we will result a fully extended curve A winding around L inside of the phase space.

Refer to Figure 13 where we depict L as a line segment and the curves L and A lying in the same plane. Although L and A are, in general, curves in three dimensional space, we can use this representation since the "sides" of L are well-defined. The way the curve A (represents $W^s(E_c)$) winds around the segment L (represents $W^u(E_j)$) charachterizes $W^u(E_j) \cap W^s(E_c)$. We will call this picture the intersection graph. Of course the intersection graph might be very complicated. Unfortunately, there is no way, except numerical experiments, to determine the real graph for the collinear three-body system. Once the graph is determined, we can "read off" the geometric structure on S^* according to Proposition 2.4(a) and Proposition 2.5.

The ideal graph is shown in Figure 14(a), where A spirals around L to create regular branches only. In this case there are no loops on S^*, and we will see in next section that the only possible strip in this case have the expression $(k, k+1, k+1)$. This gives a nice structure with the character number increase monotonically on the strips as shown in Figure 14(b).

As in Figure 15(a), intersections like a, b will give loops at Q_1 and Q_3 alternatively. A non-transversal intersection like d will give two loops at Q_1 or Q_3. Figure 15(b) shows what happens on S^* due to the intersections shown in Figure 15(a).

Figure 16(a) illustrates a more complicated situation. Again Figure 16(b) shows what happens on S^* due to the intersections shown in Figure 16(a). Again with the help of Propositions 2.4(a) and 2.5, we can look at the

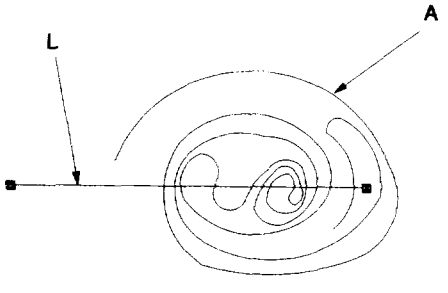

FIG. 13. The intersection graph.

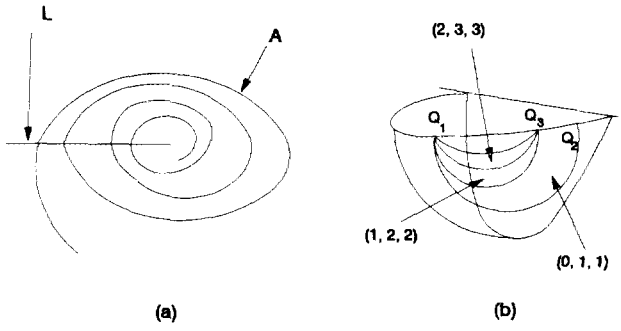

FIG. 14. The ideal intersection graph.

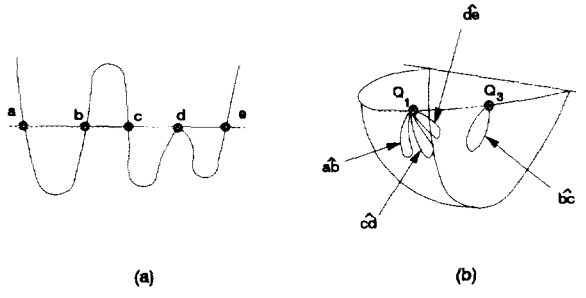

FIG. 15. Intersections that give loops.

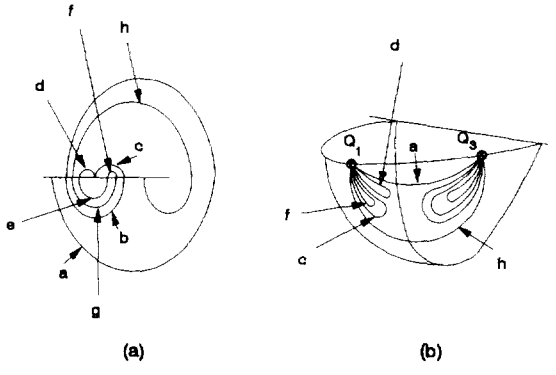

FIG. 16. Intersections give strip and loop structure.

intersection graph and transfer the information to the picture on S^*. A complicated intersection graph reflects complicated intersections of $W^u(E_j)$ and $W^s(E_c)$, therefore a complicated structure on S^*.

III. Interaction and Final Evolution

First we will look at the geometric structure at P_1 (the collision point of m_1 and m_2) and the image of S^* under the flow. Refer to Figure 17. Mimicking the construction of S at P_2, we can take a quarter sphere $\tilde{S}$ at P_1. As in this picture, $\tilde{S}^*$ is the interior of $\tilde{S}$, $\tilde{l}'$ and $\tilde{l}$ are the boundaries of $\tilde{S}^*$ on the collision manifold and the boundary $\theta = 0$ respectively (refer back to Figure 6). $\hat{\gamma}^+$, $\hat{\gamma}^-$ are two branches of $W^u(E_c)$ and $\hat{\gamma}$ is one of the branch of $W^u(E_j)$ on the collision boundary. We define

$$\tilde{Q}_1 = \tilde{\gamma}^+ \cap \tilde{l}'; \qquad \tilde{Q}_3 = \tilde{\gamma}^- \cap \tilde{l}'; \qquad \tilde{Q}_2 = \tilde{\gamma} \cap \tilde{l}'.$$

Following the flow backward, we also have four possible final evolutions: binary ejection of m_1 and m_2; triple ejection; m_1 coming in from infinity with positive velocity (hyperbolic catch); m_1 coming on from infinity with zero velocity (parabolic catch). We can define, $\tilde{H}$, $\tilde{P}$, $\tilde{E}$, analogous to H, P, E as defined in (2.1), (2.2) in Section (II), and we can define

$$\tilde{S}^* \cap \tilde{H} = \tilde{\Sigma}_H; \quad \tilde{S}^* \cap \tilde{P} = \tilde{\Sigma}_P; \quad \tilde{S}^* \cap \tilde{E} = \tilde{\Sigma}_E; \quad \tilde{S}^* \cap W^u(E_j) = \tilde{\Sigma};$$

Also, we have the corresponding definition of the character number $N(p)$ for a given point $p \in \tilde{S}^*$, but this time $N(p)$ counts the number of collisions of m_1 and m_2 for $t < 0$.

All the discussions and the results in Section II can be carried over to this new situation. So we conclude a similar geometric structure on $\tilde{S}^*$.

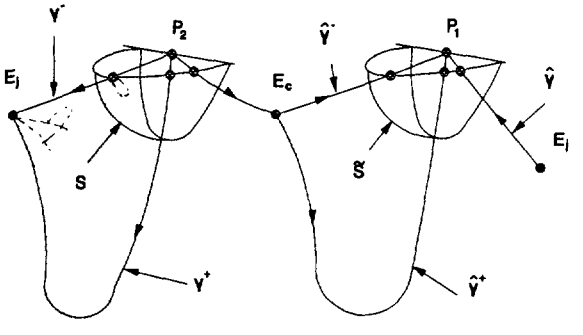

Fig. 17. The surface $\tilde{S}$ around P_1.

One sees that we can also use the same terminology as in section (II) to describe this structure. In fact, since the system is reversible, we have:

PROPOSITION 3.1. *The geometric structure on $\tilde{S}^*$ is exactly the same as that on S^*.*

If the character number for an unit U on S^* is finite, U will have an image on $\tilde{S}^*$ under the flow; denote it by $F(U)$. We see that $F(U)$ has to be an unit on $\tilde{S}^*$. Similarly, if we follow the flow backward, the image of an unit $\tilde{U}$ on $\tilde{S}^*$, which has a finite character number, will be another unit on S^*. Of course, for a unit of hyperbolic points on S^*, we can not find its image on $\tilde{S}^*$. But in this case, we can find an identical unit on $\tilde{S}^*$, which is an unit of hyperbolic catching.

For more details of the map F, we need further study the structure of the units on S. Recall that a regular curve is a simple curve connecting Q_1 and Q_3, and a loop is a simple curve with both of its ends on either Q_1 or Q_3. We will call a curve C a *basic curve* if C is either a regular curve or a loop on S.

Take a unit U on S, and a basic curve C from the interior of U. C will divide U as well as the boundary of U into two parts. Next lemma claims that for a unit U with expression $(k, k+1, k+1)$, the boundary of U consists of two consecutive parts: one with character number k and the other with character number $k+1$.

LEMMA 3.1. *For a unit U with expression $(k, k+1, k+1)$, there is a basic curve C, which divide its boundary into two consecutive parts, such that the character number of one part is k and that of the other part is $k+1$.*

We postpone the proof of this lemma for a while.

For a unit with expression $(k, k+1, k+1)$, there are three possibilities:

(a) U is a strip. One of the regular branches of the boundary has character number k. The other regular branch has character number $k+1$. We will call such a strip a *regular strip*.

(b) U is a strip. Both of the regular branches of the boundary have the same charachter number (either k or $k+1$). We will call such a strip a *strange strip*.

(c) U is a ring.

DEFINITION 3.1. For a unit U on S with expression $(k, k+1, k+1)$, take a simple curve l inside of U:

(a) l is called a *horizontal-path* if l is a basic curve, and l divides the boundary into two consecutive parts as described in Lemma 3.1.

(b) l is called a *vertical-path* if l connects two points p_1, p_2 on the boundary of U, where p_1 and p_2 have different character numbers.

For a unit with expression $(k, k+1, k)$ or (k, k, k), the definition of these two terms are easier:

DEFINITION 3.2. For a unit U on S with the representation $(k, k+1, k)$ or (k, k, k), take a curve l inside of U:

(a) l is a *horizontal-path* if l is a basic curve.

(b) l is a *vertical-path* if l connects two points on different branches of the boundary U.

Figure 18 shows typical cases of horizontal and vertical path.

DEFINITION 3.3. Take a strip U and a curve l inside of U. We call l a *vertical-curve* if l connects two points on the different regular branches of the boundary of U.

Note that we have similar definitions for units on S^*. We now have:

PROPOSITION 3.2. *Assume that U is a unit with expression $(k, k+1, k+1)$:*

(a) *If U is a regular strip, $F(U)$ will be a regular strip on S^* with the same expression.*

(b) *If U is a strange strip, $F(U)$ will be a strange strip on S^* with the same expression.*

(c) *If U is a ring at Q_1, $F(U)$ will be a strip on S^* with the expression $(k+1, k+1, k+1)$.*

(d) *If U is a ring at Q_3, $F(U)$ will be a strip on S^* with expression $(k, k+1, k)$.*

(e) *The image of a vertical-path is a regular-curve on S^* and the image of a horizontal-path is a vertical-curve on S^*.*

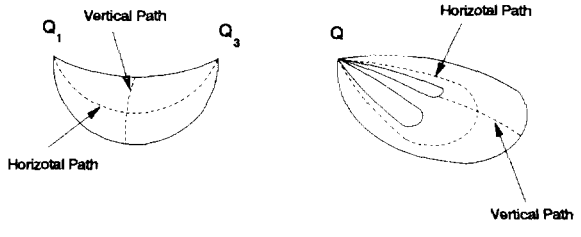

FIG. 18. The horizontal and vertical path.

Also, we have similar results for units with expression $(k, k+1, k)$ and (k, k, k):

PROPOSITION 3.3. (a) *If U is a strip with expression (k, k, k), $F(U)$ will be a ring at $\tilde{Q}_1$ with expression $(k-1, k, k)$.*

(b) *If U is a strip with expression $(k, k+1, k)$, $F(U)$ will be a strip at $\tilde{Q}_3$ with expression $(k, k+1, k+1)$.*

(c) *F maps regular-curve to vertical-path and vertical-curve to horizontal-path.*

PROPOSITION 3.4. (a) *If U is a ring at Q_1 with expression $(k, k+1, k)$, $F(U)$ will be a ring at $\tilde{Q}_3$ with expression $(k+1, k+1, k+1)$.*

(b) *If U is a ring at Q_1 with expression (k, k, k), $F(U)$ will be a ring at $\tilde{Q}_1$ with the expression (k, k, k).*

(c) *If U is a ring at $\tilde{Q}_3$ with expression $(k, k+1, k)$, $F(U)$ will be a ring at $\tilde{Q}_3$ with expression $(k, k+1, k)$.*

(d) *If U is a ring at Q_3 with expression (k, k, k), $F(U)$ will be a ring at $\tilde{Q}_1$ with expression $(k-1, k, k-1)$.*

(e) *The image of a vertical-path is a horizontal-path, and that of a horizontal-path is a vertical-path.*

Proposition 3.2–3.4 provide a detailed correspondence between the units on S and S^*. Furthermore, the last statement from each of these propositions described certain "hyperbolic behavior" of the flow-defined map. Although no metric is involved on S and S^*, we can still recognize the "hyperbolicity" topologically: each horizontal-path is "compressed" and each vertical-path is "stretched" by the flow defined map F. Refer to Figure 19, where a regular strip with expression $(k, k+1, k+1)$ is presented. B_1 represents all the boundary branches with character number $k+1$, and B_2 represents that with character number k. From S to S^*, the horizontal-paths are "compressed" and

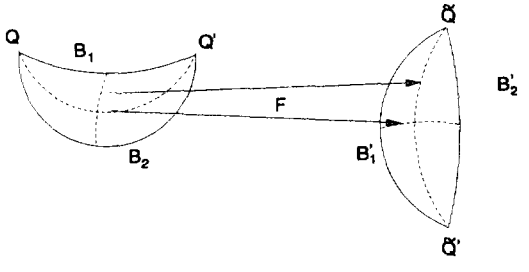

FIG. 19. The action on a unit.

the vertical-paths are "stretched". As an extreme case, two points, Q and Q', are "stretched" to become two lines. Meanwhile, two lines, B_1 and B_2 are compressed to two points, $\tilde{Q}$ and $\tilde{Q}'$ respectively.

One see that this "hyperbolic" behavior of the mapping F from S to S^* implies, potentially, complicated dynamic phenomenon. It corresponds to the first step to construct a horseshoe. To complete the construction, one need to overlap the image on S^* back on the original units. This is exactly what the regularization of binary collision of m_1 and m_2 will accomplish. Now turn to the proof of all these claims we have made in this section:

Proofs of Lemma 3.1 *and Proposition* 3.2–3.4. We have many claims in Proposition 3.2–3.4, but fortunaltely the argument are similar for most of the cases involved. In fact, we are going to provide a basic geometric picture behind all of the claims as well as their proofs.

The overall picture is Figure 17, where all the rest points and the connections among them are depicted. Take a loop l with two tails $T_1 < T_2$ at Q_1. Remember that l is on $W^s(E_c)$. We see that, following the flow, l will go with γ^+ first. When it "reaches" E_j, the tails of the loop will split. T_1 will go with l_{T_1}, and T_2 with l_{T_2}. Now the situation is as in Figure 12, where B_0 is the image of the loop l, $p = l_{T_1} \cap L$, $p = l_{T_2} \cap L$.

Stay with Figure 12. Following the flow, the loop B_0 will become $p'p'_1$ and finally converge to E_c. Meanwhile, the arc pp_1 on L will become a curve connecting p' and p'_1 nearby E_c. This arc will keep going to meet S^* where it will become boundaries for units on S^*.

As a example, we take a ring at Q_1 on S. To simplify the discussion, we assume that the number of its inner loops is finite. Take the curve L again as in Figure 12. As described above, every boundary loop will go along γ^+ in Figure 17 first, then split on $W^u(E_j)$ according to Proposition 2.4(c). Together with Proposition 2.4(a), we will have Figure 20 for what is between E_j and E_c. The straight line stands for L and all the arcs stand for the image of boundary loops. Also, by Proposition 2.4(b), all of the dots

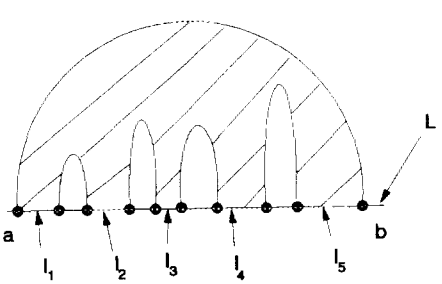

FIG. 20. The image of a ring under the flow.

on L are in $W^u(E_j) \cap W^s(E_c)$, and the shaded area is the interior of the ring.

The boundary of the shaded area consists of all the arcs and *a set of intervals of* L. One see that, with the flow, all the arcs will converge to E_c, and all these intervals of L on the boundary will go forward to form the new boundary of a unit on S^*, which is the image of our original ring on S.

Now let us have a closer look at these intervals of L on the boundary. Denote such an interval as $[c, d]$, where c, d are end points. Again we can associate a triplet (k_1, k_2, k_3) to $[c, d]$. $k_1 \leqslant k_3$ stands for the character number of c and d, and k_2 for the character number of the interior of $[c, d]$. We will still have restrictions $k_1 \leqslant k_3 \leqslant k_2 \leqslant k_1 + 1$. So the only feasible triplets are (k, k, k), $(k, k+1, k)$, $(k, k+1, k+1)$.

For the case of (k, k, k), both ends of the interval will go along $\hat{\gamma}^-$ in Figure 17 after reaching E_c. So its image will be a loop at $\tilde{Q}_1$ on S^*. It is not the case for the case of $(k, k+1, k)$. After reaching E_c, the interior points close to c and d on $[c, d]$ have experienced only k binary collisions between m_2 and m_3. Following $\hat{\gamma}^-$ never contributes another binary collision of m_2 and m_3 to the solution. So both of the ends will go along $\hat{\gamma}^+$. This will give a loop at $\tilde{Q}_3$ on S^*. Similarly, an interval with triplet $(k, k+1, k+1)$ will give a *regular curve* on S^*.

Here comes the argument for Lemma 3.1: Since a unit on S^* has either two (strip) or none (ring) regular branches on its boundary, we will have, correspondingly, two or none such intervals we just described with triplet $(k, k+1, k+1)$. For a unit on S with expression $(k, k+1, k+1)$, the otherwise case of this lemma will give more than two such intervals, so will induce contradiction.

One can see the motivation for the definitions of horizontal and vertical path. In the case of a unit $(k, k+1, k+1)$, a horizontal-path is a curve, such that following the flow as in the situation of Figure 20, it becomes a curve connecting the two intervals on L with triplet $(k, k+1, k+1)$. It is easy to see that its image will be a vertical-curve on S^*.

With all these pictures in mind, more detailed correspondences between S and S^* could be obtained. They are all listed in Proposition 3.2–3.4. ∎

Now we will regularize the binary collision of m_1 and m_2. Recall the McGehee's manifold in Figure 6. We will consider the case of $\mu = 1$ at first.

By regularizing the binary collision of m_1 and m_2, we introduce a map from $\tilde{S}^*$ to S^*. Denote this map by R. R corresponds to the second step in the construction of a standard horseshoe map--the overlap of $\tilde{S}^*$ on S^*.

Refer to Figure 21. According to the flow on McGehee's manifold, we will have P_1, P_3 on l'. P_3 is on the arc $Q_1 Q_3$ and P_1 is on $Q_2 b$. Where $P_1 = R(\tilde{Q}_1)$, $P_3 = R(\tilde{Q}_3)$.

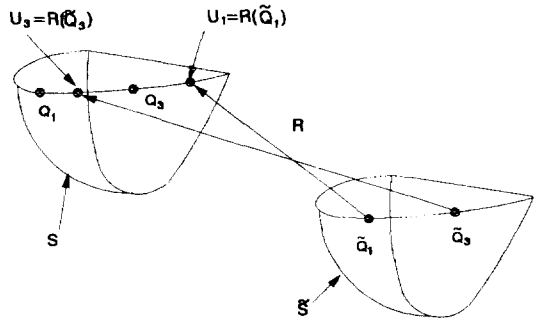

FIG. 21. The action of R.

Now take strips $(k, k+1, k+1)$ on S^* for all the positive integers k and denote it by U_k. $F(U_k)$ will be a strip on $\tilde{S}^*$ with expression $(k, k+1, k+1)$ by Proposition 3.5(a). Under the map R, $F(U_k)$ becomes a strip V_k, which overlaps all the U_i's on S^* as shown in Figure 22.

This structure implies a symbolic system with all of the positive integers as its alphabet set in the usual manner. In fact this picture will also give periodic solutions and much more.

Note that we only considered a part of the strips and their image in this picture. The actual structure on S^* might also include strips with the expression $(k, k+1, k)$ and (k, k, k) as well as the possible rings. So the overlap introduced by R will cause a situation which will be far more complicated than the typical horseshoe map. Analytically, one can even give the first order estimation of the map R. (By introduce S^* and $\tilde{S}^*$ identically, and treat the regularization as an elastic bounce). But this won't help to improve our understanding of the map $R^{\circ}F$ because we can do very little to determine the details of the geometric structure on S^* analytically.

One does not always get the typical horseshoe illustrated in Figure 22 for the collinear three-body problem. For most of the combinations of masses,

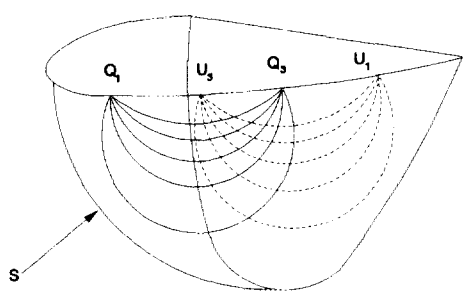

FIG. 22. Horseshoe map in the case of $\mu = 1$.

$\mu > 1$. In this case, $R(\tilde{Q}_1)$ and $R(\tilde{Q}_3)$ will land on the arc $Q_2 b$. So the overlap in Figure 22(a) does not happen. However, we can track the image of $\tilde{Q}_1$ and $\tilde{Q}_3$ under the iteration of $R^{\circ}F$ as many times as we want, and read the images directly from McGehee's manifold. We see that, referring to Figure 6, finally $(R^{\circ}F)^{\mu}(\tilde{Q}_1)$ will be in the arc $Q_1 Q_3$ and $(R^{\circ}F)^{\mu}(\tilde{Q}_3)$ will be in the arc $Q_2 b$.

It is unfortunate that when we iterate $R^{\circ}F$, we have no control on the image of the rest of the strip $F(U_k)$. It would be very nice if all of the $(R^{\circ}F)^{i}(U_k)$ were elliptic points. Where $0 < i \leqslant \mu$. The horseshoe illustrated in Figure 22 would happen for the map $(R^{\circ}F)^{\mu}$. But it does not seem to be the case.

Although the whole picture on S^* might be very complicated and very hard to handle for the case of $\mu > 1$, the existence of a symbolic system in this problem is not as hard to establish—we do not even need much of the discussions in Sections II and III. A detailed argument will be presented elsewhere.

REFERENCES

1. J. N. MATHER AND R. MCGEHEE, "Solution for Collinear Four Body Problem which Becomes Unbounded in Finite Time," Lecture Notes in Physics, Vol. 3, pp. 573–597. Springer-Verlag, New York, 1975.
2. D. SAARI AND Z. H. XIA, Oscillatory and super-hyperbolic solutions in Newtonian system, *J. Differential Equations* **82** (1988), 342–355.
3. K. R. MEYER AND Q. D. WANG, The global phase structure of the restricted isosceles three-body problem with positive energy, *Trans. Amer. Math. Soc.*, to appear.
4. K. R. MEYER AND Q. D. WANG, The global phase structure of the three-dimensional isosceles three-body problem with zero energy, *in* "Hamiltonian Dynamical Systems: Theory, History, and Aplications" (S. Dumas, K. R. Meyer, and D. S. Schmidt, Eds.), IMA Proceedings Series, Springer-Verlag, New York, to appear.
5. Q. D. WANG, The global solution of the N-body problem, *Celestial Mech.* **50** (1991), 73–88.
6. R. MCGEHEE, Triple collision in the collinear three-body problem, *Invent. Math.* **27** (1974), 191–127.
7. R. MCGEHEE, A stable manifold theorem for degenerate fixed points with applications to celestial mechanics, *J. Differential Equations* **14** (1973), 70–88.